Research Article **Open Access**

Ali S. Basaham, Ibrahim M. Ghandour*, and Rabea Haredy

Controlling factors on the geochemistry of Al-Shuaiba and Al-Mejarma coastal lagoons, Red Sea, Saudi Arabia

https://doi.org/10.1515/geo-2019-0034
Received December 24, 2018; accepted June 26, 2019

Abstract: Geochemical and mineralogical analyses of bottom sediments collected from Al-Shuaiba (SHL) and Al-Mejarma (MJL) coastal lagoons, Red Sea were carried out. Mineralogically, the sediments consist mainly of carbonate minerals particularly aragonite, high and low Mg-calcite and traces of dolomite admixed with non-carbonate minerals including quartz, k-feldspars, plagioclase and traces of amphiboles, mica and clay minerals. The spatial distribution of major and trace elements at the bottom of the lagoons indicates two groups of elements. The first, less significant, is of terrigenous origin concentrates mainly in the shoreward direction. This group includes the silicates (Al_2O_3-Fe_2O_3-SiO_2), Feldspars (K_2O-Rb-Ba) and heavy minerals (V-Cr-Zr, TiO_2-Y-Nb) related elements. The second most dominant group is the carbonate related elements (CaO-Sr) that concentrates in the seaward direction. The two lagoons are not affected by urbanization or anthropogenic impact, and hence the siliciclastic elements are related to the terrigenous influx mainly by aeolian transportation. The carbonate related elements are mainly of biogenic origin related to calcareous skeletal remains. The elemental distribution in the bottom sediments of the MJL is more homogeneous than those in the SHL reflecting the bottom conditions that are mainly controlled by lagoon morphology, hydrodynamic and the water circulation between the lagoon and the sea. Geochemical data show no obvious enrichment of Al-normalized redox-sensitive trace elements V and Cr suggesting that there is no variation in the bottom redox conditions in contrast with other previous studies. The information in this work is an important tool for biogeochemical and biological research projects in the Red Sea coastal lagoons.

Keywords: Al-Shuaiba and Al-Mejarma lagoons, bottom sediment geochemistry, bottom redox conditions, cluster analysis, geochemical association

1 Introduction

Coastal lagoons are worldwide socio-economically fragile ecosystems of high biological productivity and nutrients availability, covering a wide variety of habitats and host abundant fauna and flora constituting a vital and important fishery and nursery ground [1, 2]. Several proxies have been employed to study the bottom conditions of coastal lagoons; however, bottom sediment geochemistry is still the most powerful and effective proxy. Lagoonal bottom sediments are archives for environmental and climatic fluctuations and aid in forecasting the future of the ecosystem. The bottom sediments are derived from different sources including continental run-off, coastal erosion, upwelling and resuspension, reworked marine sediments and autochthonous biogenic carbonate and hydrogenous sediments. Physical, chemical and biological processes in the lagoon act mutually or individually on the transport and deposition of sediments affecting the chemical composition of bottom sediments [3, 4]. In addition, lagoon hydrodynamics largely control water quality conditions, regulate sediment dispersal patterns, their subsequent deposition and mixing with autochthonous sediments [5].

There are over twenty elongated and shallow lagoons locally known as sharms and/or Khawrs extending along

Ali S. Basaham, Rabea Haredy: Marine Geology Department, Faculty of Marine Science, King Abdulaziz University, P.O. Box 80207, Jeddah 21589, Saudi Arabia
***Corresponding Author: Ibrahim M. Ghandour:** Marine Geology Department, Faculty of Marine Science, King Abdulaziz University, P.O. Box 80207, Jeddah 21589, Saudi Arabia,
E-mail: ighandour@kau.edu.sa
Geology Department, Faculty of Science, Tanta University, Tanta 31527, Egypt

the Saudi the Red Sea coast [6]. These lagoons have gently sloping shorelines and connect to the Red Sea through one or more inlets. The existence and evolution of Red Sea coastal lagoons are related either to the rise of sea level (RSL) during the Holocene [7] or as remnants of collapse features formed by selective dissolution of Miocene evaporites [8]. The description of the sedimentological characteristics and the composition of bottom sediments of major Red Sea coastal lagoons were reviewed by Rasul [6]. The extreme arid climate with a very limited and negligible annual rainfall and therefore, the composition of the lagoon bottom sediments are dominantly of autochthonous biogenic sediments. The geochemistry of the Red Sea coastal lagoons has been examined by many investigators mainly for environmental assessments. Most of previous studies concentrated in the lagoons surrounding major cities; Jeddah [9], Rabigh [10–13] and Yanbu [14].

Al-Shuaiba (SHL) and Al-Mejarma (MJL) lagoons on the eastern coast of the Red Sea, Saudi Arabia (Fig. 1) lack major industrial activity and the anthropogenic contribution is very limited to slight fishing activities. The two lagoons show variable morphologies and connection with the Red Sea producing different hydraulic circulation within the two lagoons and consequently different physical and biogeochemical processes, dispersal patterns and composition of bottom sediments. The lagoons were previously studied for their sedimentological and micropaleontological attributes [15–19]. The geochemistry of the environmentally sensitive elements in the bottom sediments of the two lagoons were involved to establish a geochemical background for the Red Sea coastal lagoons [11].

The present study is a part of an ongoing research project on the geochemistry of the Red Sea coastal lagoons. Basaham et al. [11] published a part of the data to establish a geochemical background for the Red Sea coastal lagoon sediments. The aims of the present study are to map the elemental distribution in the carbonate dominated Al-Shuaiba and Al-Mejarma lagoons to determine the sources and pathways of the elements in the lagoons and to understand the controlling factors on their spatial distribution. The findings of this work will be employed as important information for future biogeochemical and biological research projects in the carbonate rich Red Sea coastal lagoons.

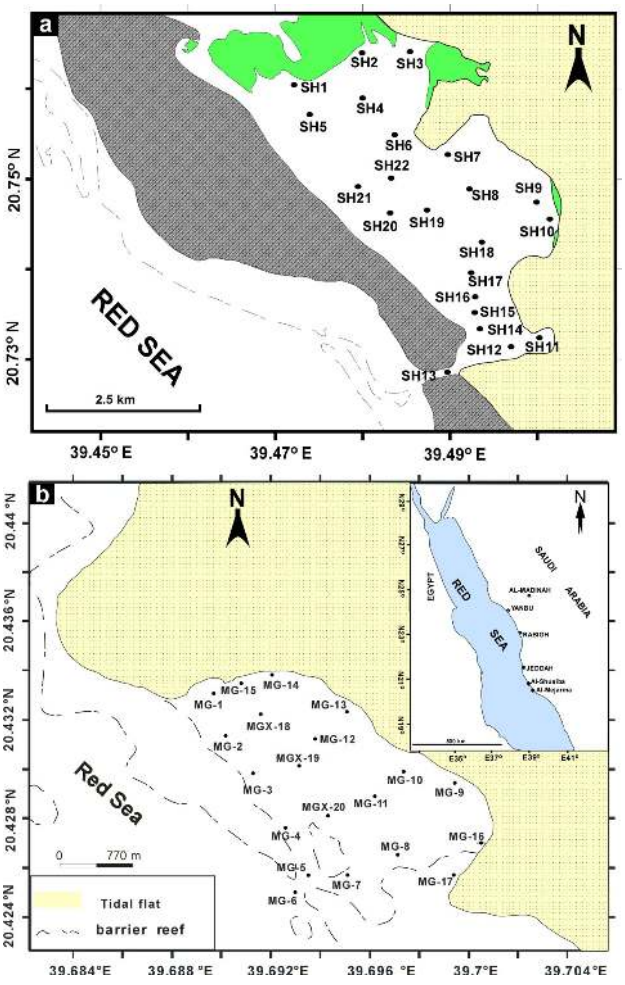

Figure 1: Locations of Al-Shuaiba (a) and Al-Mejarma (b) lagoons and the sampling sites.

2 Materials and Methods

2.1 Area of Study

Al-Shuaiba (Khawr ash Shaiba Al Maftuhah) Lagoon (SHL) is a fossil back-reef and hypersaline small basin located 80 km south of Jeddah city between latitudes 20° 42′ to 20° 51′ N and longitudes 39° 26′ to 39° 32′ E. It is a type of choked lagoon [20] connected to the sea through an elongated inlet channel with depth up to 15 m. The lagoon has an irregular shape and their bottom topography is relatively smooth with shallow depth varying from 1 to 3 m. It covers a surface area of about 14.3 km^2. The lagoon contains mangrove trees (*Avicennia marina*) scatter around the margins of the lagoon and the small islands appearing within the lagoon, whereas the eastern side is bordered by a low-lying and extensive mud-rich tidal flat. The western side of the lagoon is bordered by old, raised coral reef terraces

(1-3 m high); probably of Pleistocene age [21, 22]. Rainwaters rarely drain into the lagoon through the generally inactive Wadi Al-Atwa, Wadi Al-Kharqah and unknown wadi during the sporadic major floods [6]. The composition and the grain size of bottom sediments vary widely in the lagoon. The bottom sediments consist dominantly of coarse grained autochthonous carbonates dominated by biogenic corals and molluscan remains commonly occur within the high energy channel course of the lagoonal entrance admixed with terrigenous sediments transported to the lagoon by wind action and less evaporite minerals derived from the adjacent sabkha. Fine grained sediments are common in the sheltered and low energy nearshore areas. In addition, the bottom of the lagoon is occupied by sea grasses and macro-algae [17].

Al-Mejarma Lagoon (MJL) is a back-barrier lagoon situated about 40 km south of Al-Shuaiba at latitudes N 20° 25′29″, N 20° 26′4.02″ and longitudes E 39° 41′23″, and E 39° 42′4″. The lagoon occupies an area of 0.88 km^2 and has a more regular rectangular shape with long axis (1.4 km long) parallel to the Red Sea shoreline. The water depth of the MJL varies from 1 to 7 m with an average of 2.5 m and it is connected to the open sea through a narrow channel about 70 m width and 7 m depth. The bottom topography is smooth except for the presence of some patchily distributed coral reefs. The water dynamic is variable, energetic along the channel and very calm on both northern and southern part. The bottom sediments is generally heterogeneous. Coarse biogenic sediments containing remains of corals and molluska are abundant in the high energy along the inlet channels, whereas muddy sands with abundant seaweeds consisting of algae and foraminifera admixed with wind-transported terrigenous sediments. The lagoon is surrounded to the south and north by low lying intertidal flat and coastal sand dunes and to the east by beachrocks.

2.2 Climate

The area has a hot and dry climate throughout the year with a very low precipitation rate (< 63 mm/yr) and high evaporation rates (2.06 ± 0.22 m/yr) with no riverine inputs [23]. The lagoons have a semidiurnal low tidal range about 0.3 m that is similar to that of the central Red Sea [24]. The energy flux generated by wind-generated waves and currents along with tidal currents control the sediment transportation at the entrance of the lagoon [6, 25]. The water circulation between the lagoons and Red Sea is of reversal estuarine type. It is maintained by the narrow inlets that allow the formation of two water layers; the cold and less saline Red Sea waters enter the lagoons as surface layer (inflow) and warm and high salinity lagoonal waters leave the lagoon as subsurface layer (outflow). The water circulation is governed mainly by wind, tide and thermohaline circulation [17, 26, 27]. The shallow depths, and wind and tidal stirring prevent the lagoons from developing stratification, resulting in a well-mixed oxygenated body of water.

2.3 Database and Methodologies

The database of the present study includes the mineralogical and geochemical analysis of 42 samples of bottom sediments collected in February, 2014 by the van Veen-type grab sampler from Al-Shuaiba (22 samples) and Al-Mejarma lagoons (20 samples) (Fig. 1). The samples were dried at 50°C and gently powdered. Mineralogical and geochemical compositions were determined using XRD and XRF techniques, respectively. The bulk mineralogy of 12 samples (10 from Al-Mejarma and 2 from Al-Shuaiba) was determined using the X-ray powder diffraction (XRD) (SHIMZU) with Ni-filtered Cu Kα radiation at 15 kV to 40 mA at the XRD Laboratory of the Marine Geology Department, King Abdulaziz University. The relative abundance of minerals is determined semi-quantitatively using the peak heights of the basal reflections for the mineral [28, 29]. The identified minerals are grouped into abundant (> 40%), moderate (10 – 40 %) and trace (< 10%). The chemical composition of sediments was determined using a RIGAKU RIX 2100 X-ray fluorescence spectrometer (XRF), equipped with Rh/W dual-anode X-ray tube. The measurements were performed at the Department of Geosciences, Osaka City University, Japan under 50 kV and 50 mA accelerating voltage and tube current, respectively [30]. Fused glass discs were prepared by mixing 1.8 g of powdered sample (dried to 110°C for 4 hours), 3.6 g of spectroflux ($Li_2B_4O_7$ 20%, $LiBO_2$ 80%, dried at 450°C for 4 hours), 0.54 g of oxidant $LiNO_3$ (dried at 110°C for 4 hours) and traces of LiI. The mixture is then fused at 800°C for 120 sec and 1200°C for 200 sec. The accuracy of the analyses was estimated to be ±2-3 % for major elements and ±10-15 % for trace elements. Total iron is introduced as $Fe_2O_3{}^t$. For comparison, the chemical composition of the bottom sediments of Sharm Al-Kharrar (unpubl. Data) and Sharm Obhur [9] have been used. Descriptive statistics and the elemental interrelationships are determined and the spatial distribution of major oxides and trace elements are shown by contour maps. The chemical variables in the sediments of SHL and MJL are clustered using corre-

lation coefficients as a similarity index [13, 31] with the aid of PAST 3.11 [32].

3 Results

3.1 Mineralogical Composition

The mineralogical composition of the SHL and MJL bottom sediments supplemented with data from previous work [16] show that the mineralogical composition consists mainly of carbonate minerals, particularly high Mg-calcite (HMC), aragonite, low Mg-calcite and traces of dolomite. In addition, non-carbonate terrigenous minerals including quartz, k-feldspars, plagioclase, amphiboles, mica and clay minerals.

3.2 Geochemistry

The results of the geochemical analysis are shown in tables (1-4) and figures (2-5).

3.2.1 Major elements

The distribution of the terrigenous related major elements (SiO_2, TiO_2, Al_2O_3, Fe_2O_3, MnO and Na_2O) differs from the carbonate related ones (CaO and MgO). The concentrations of the former increase shoreward particularly towards the eastern shoreline (Figs 2 and 4). The ranges of concentrations of SiO_2, TiO_2, Al_2O_3 and Fe_2O_3 in the sediments of Al-Shuaiba and Al-Mejarma lagoons are 11.63-25.44, 0.25-0.77, 3.46-6.53 and 1.78-3.35 % and 13.09-40.12, 0.23-1.04, 3.79-11.44 and 1.56-6.08 %, respectively (Tables 1 and 2). The CaO and MgO have a unique aerial distribution, where they are highly enriched adjacent to the inlet and in the areas mostly attached to the open sea (Figs 2 and 4). The concentrations of CaO varied in the sediments of Al-Shuaiba Lagoon between 45.48 and 61.56 % with an average of 56.29 % and in Al-Mejarma Lagoon from 26 to 60 % with an average of 49 % (Tables 1 and 2). MgO concentrations on the other hand display north and westward increase in the sediments of Al-Shuaiba, whereas the highest concentrations of the MgO in the sediments of Al-Mejarma were recorded from the nearshore area adjacent to the southern shoreline. Its concentration varied in the sediments of Al-Shuaiba from 4.61 to 6.93 % with an average of 5.69 % and from 4 to 8.1 % with an average of 5.1 % in the sediments of Al-Mejarma Lagoon. K_2O and P_2O_5 in

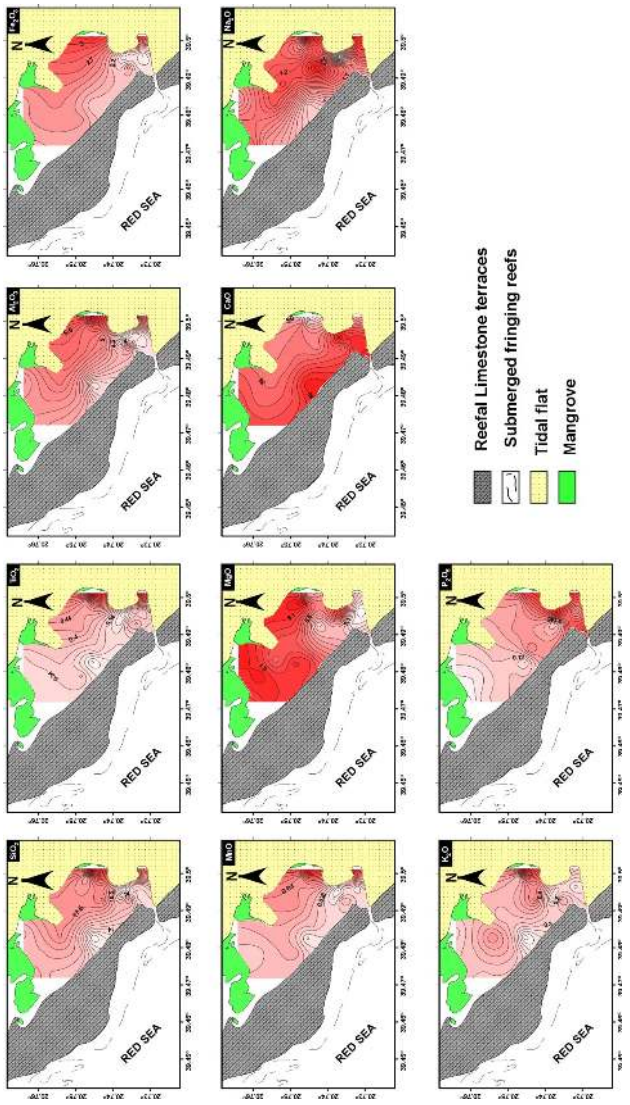

Figure 2: Contour maps showing the spatial distribution of major oxides (%) in the bottom sediments of Al-Shuaiba Lagoon

the sediments of Al-Shuaiba behave slightly different from other major elements. The concentration of K_2O in the sediments of Al-Shuaiba and Al-Mejarma lagoons varied from 0.2 to 0.7 % and from 0.42 to 1.32 % displaying an increase towards eastern central part of the lagoon. P_2O_5 concentration on in the sediments of Al-Mejarma shows a similar trend to the terrigenous related elements, whereas its concentration in the sediments of Al-Shuaiba increases in the southeast direction (Fig. 2). The concentration of P_2O_5 ranged from 0.1 to 0.19 % (average; 0.14 %) in Al-Shuaiba, and 0.17 to 0.34 % (average 0.24 %) in Al-Mejarma.

Table 1: The results of geochemical analysis of the Al-Shuaiba Lagoon bottom sediments

Sample	Major oxides (wt %)										Trace elements (μg/g)										
	SiO_2	TiO_2	Al_2O_3	T-Fe_2O_3	MnO	MgO	CaO	Na_2O	K_2O	P_2O_5	V	Cr	Ni	Cu	Zn	Rb	Sr	Y	Zr	Nb	Ba
SH-1	16.24	0.33	4.76	2.26	0.04	5.96	57.74	1.16	0.32	0.10	57	42	18	32	30	4	5336	10	185	4	91
SH-2	15.79	0.34	4.82	2.38	0.04	6.10	57.61	1.12	0.32	0.10	64	42	13	35	29	4	5396	10	183	4	99
SH-3	15.34	0.34	4.66	2.36	0.04	6.31	56.74	1.02	0.29	0.11	57	37	15	33	34	4	5241	10	188	4	97
SH-4	16.02	0.33	4.91	2.47	0.04	6.28	55.36	1.12	0.34	0.11	53	39	17	31	30	6	5102	9	170	3	103
SH-5	15.42	0.33	4.70	2.34	0.04	6.14	57.14	1.05	0.32	0.11	56	36	37	30	29	5	5350	9	175	4	97
SH-6	17.58	0.36	5.11	2.51	0.04	5.74	54.86	1.19	0.42	0.12	60	41	16	28	31	6	5177	10	183	4	111
SH-7	17.94	0.39	5.27	2.60	0.04	5.82	54.20	1.23	0.33	0.13	63	37	31	31	31	5	5199	12	198	4	101
SH-8	17.65	0.43	5.26	2.68	0.04	5.93	54.77	1.21	0.36	0.14	58	43	14	32	32	6	5227	11	228	4	116
SH-9	16.55	0.45	5.30	2.95	0.04	6.39	54.12	1.06	0.34	0.14	68	47	19	35	38	5	5325	11	284	4	74
SH-10	25.44	0.75	6.53	3.20	0.06	5.14	45.48	1.38	0.70	0.17	78	57	16	24	38	14	4114	17	442	6	179
SH-11	22.03	0.77	6.02	3.35	0.06	5.32	49.07	1.34	0.38	0.19	92	65	14	34	37	5	5738	19	498	6	127
SH-12	14.23	0.34	3.91	1.78	0.03	4.61	59.08	1.21	0.25	0.14	47	31	8	29	21	3	6537	9	243	3	89
SH-13	13.49	0.31	4.00	2.04	0.03	5.41	61.14	0.95	0.30	0.19	53	40	11	38	33	4	6456	10	221	3	81
SH-14	14.02	0.41	3.92	1.99	0.04	4.78	59.12	1.08	0.33	0.16	56	44	10	32	24	5	6367	11	302	3	69
SH-15	11.63	0.26	3.46	1.78	0.03	6.15	61.56	0.79	0.27	0.19	50	41	12	35	34	6	5858	7	194	3	62
SH-16	16.75	0.38	4.81	2.37	0.04	5.20	55.24	1.15	0.37	0.13	67	42	13	33	32	5	6246	11	238	4	76
SH-17	14.86	0.29	4.29	2.03	0.03	5.29	56.88	1.16	0.24	0.12	48	33	11	29	23	2	5809	8	180	3	98
SH-18	18.69	0.36	4.99	2.47	0.04	4.90	53.50	1.35	0.45	0.14	59	42	7	28	23	8	5040	10	186	4	117
SH-19	14.84	0.35	4.45	2.25	0.04	5.62	59.30	1.03	0.31	0.14	57	40	14	35	29	4	5808	10	231	4	90
SH-20	11.89	0.25	3.89	2.10	0.03	6.05	60.84	0.93	0.20	0.11	56	36	14	33	31	1	6199	8	177	3	68
SH-21	15.56	0.36	4.69	2.43	0.04	6.01	57.39	0.98	0.34	0.12	64	41	15	34	35	6	5831	10	224	4	90
SH-22	15.35	0.32	4.71	2.35	0.04	6.13	57.33	1.04	0.35	0.12	58	38	15	30	31	5	5422	9	179	4	100
Min	11.63	0.25	3.46	1.78	0.03	4.61	45.48	0.79	0.20	0.10	47.30	30.60	7.00	24.10	20.90	1.10	4114.00	7.40	169.70	2.90	62.10
Max	25.44	0.77	6.53	3.35	0.06	6.39	61.56	1.38	0.70	0.19	92.00	65.30	37.20	38.20	38.00	13.70	6537.10	18.70	497.80	5.90	178.60
Mean	16.24	0.38	4.75	2.40	0.04	5.69	56.29	1.12	0.34	0.14	60.11	41.49	15.44	31.91	30.58	5.15	5580.91	10.50	232.27	3.88	97.04
Sta.dev.	3.05	0.13	0.71	0.40	0.01	0.53	3.76	0.14	0.10	0.03	10.02	7.45	6.78	3.17	4.72	2.37	571.31	2.71	84.98	0.74	24.73

Table 2: The results of geochemical analysis of the Al-Mejarma Lagoon bottom sediments

Sample	Major oxides (wt %)										Trace elements (μg/g)										
	SiO_2	TiO_2	Al_2O_3	T-Fe_2O_3	MnO	MgO	CaO	Na_2O	K_2O	P_2O_5	V	Cr	Ni	Cu	Zn	Rb	Sr	Y	Zr	Nb	Ba
MG-1	18.55	0.35	5.50	2.54	0.04	5.07	52.15	1.45	0.42	0.20	52	36	14	36	37	7	5555	13	196	5	141
MG-2	15.05	0.30	4.05	1.70	0.03	3.98	58.50	1.27	0.50	0.18	40	23	2	30	20	10	6356	11	239	4	127
MG-3	14.75	0.26	4.32	1.87	0.03	4.63	58.08	1.18	0.49	0.18	39	26	8	32	27	12	5969	10	184	4	110
MG-4	14.14	0.25	4.13	1.81	0.03	4.71	58.28	1.23	0.43	0.19	41	27	9	33	25	7	5773	3	186	4	119
MG-5	16.31	0.33	5.31	2.65	0.04	5.97	54.22	1.03	0.49	0.28	50	43	18	39	45	12	5031	12	165	5	118
MG-6	14.85	0.29	4.63	2.25	0.03	5.68	56.96	1.02	0.50	0.24	48	32	12	37	38	12	5311	11	166	5	99
MG-7	13.09	0.23	3.79	1.56	0.03	4.62	60.26	1.16	0.43	0.17	35	26	5	32	21	8	5954	9	180	3	113
MG-8	28.16	0.81	8.03	3.92	0.08	5.01	41.32	1.79	0.89	0.33	73	52	21	32	53	22	4268	27	474	10	217
MG-9	30.06	0.74	8.58	4.00	0.08	5.09	39.61	1.78	1.06	0.28	86	53	21	33	58	28	4150	26	513	9	231
MG-10	22.03	0.43	6.29	2.84	0.05	4.83	49.60	1.44	0.80	0.22	59	41	15	33	41	20	5193	16	252	6	173
MG-11	21.26	0.46	6.20	2.88	0.05	4.69	50.36	1.40	0.78	0.23	65	46	19	36	42	19	5318	16	274	6	158
MG-12	19.40	0.37	5.59	2.52	0.04	4.52	52.65	1.40	0.66	0.21	52	37	12	33	34	16	5487	14	219	5	150
MG-13	32.04	0.83	9.17	4.45	0.08	5.28	36.00	1.94	1.00	0.31	87	61	26	36	63	22	3765	28	474	10	227
MG-14	21.83	0.43	6.35	2.95	0.05	4.56	48.90	1.63	0.60	0.21	60	53	17	48	46	12	5638	14	235	6	158
MG-15	19.61	0.37	5.92	2.72	0.04	5.00	50.90	1.49	0.51	0.20	54	40	12	44	42	8	5427	13	187	5	151
MG-16	40.12	1.04	11.11	5.40	0.10	6.38	25.97	2.25	1.32	0.34	105	77	34	30	77	33	2268	34	722	12	310
MG-17	36.86	0.91	11.44	6.08	0.10	8.08	27.00	1.93	1.16	0.33	107	77	40	42	101	33	2334	30	537	12	269
MG-18	17.04	0.29	4.74	1.96	0.04	4.13	55.56	1.41	0.48	0.19	41	25	6	35	25	9	5961	11	210	4	142
MG-19	19.90	0.38	5.96	2.76	0.05	4.93	51.83	1.39	0.71	0.22	54	37	14	30	42	18	5315	13	202	5	171
MG-20	22.10	0.41	6.39	2.76	0.05	4.76	49.53	1.52	0.80	0.22	52	37	13	30	39	22	5016	15	214	6	176
Min	13.09	0.23	3.79	1.56	0.03	3.98	36.00	1.02	0.42	0.17	35	23	2	30	20	7	3,765	3	165	3	99
Max	32.04	0.83	9.17	4.45	0.08	5.97	60.26	1.94	1.06	0.33	87	61	26	48	63	28	6,356	28	513	10	231
Mean	20.01	0.42	5.83	2.67	0.05	4.86	51.37	1.42	0.64	0.23	55	39	13	35	39	15	5,305	15	254	6	154
Sta dev	5.49	0.19	1.53	0.80	0.02	0.48	6.74	0.25	0.21	0.04	15	11	6	5	12	6	677	6	111	2	40

Table 3: Correlation matrix of major and trace element concentrations for the bottom sediments of Al-Shuaiba Lagoon. All correlations are significant at the P < 0.01 level (n = 22).

	SiO_2	TiO_2	Al_2O_3	$^tFe_2O_3$	MnO	MgO	CaO	Na_2O	K_2O	P_2O_5	V	Cr	Ni	Cu	Zn	Rb	Sr	Y	Zr	Nb	Ba
SiO_2	1																				
TiO_2	0.88**	1																			
Al_2O_3	0.95**	0.82**	1																		
$^tFe_2O_3$	0.87**	0.84**	0.96**	1																	
MnO	0.9**	0.92**	0.88**	0.88**	1																
MgO	-0.39	-0.3	0.01	0.11	-0.10	1															
CaO	0.98**	0.87**	0.95**	-0.9**	0.87**	0.18	1														
Na_2O	0.84**	0.66**	0.75**	0.61**	0.64**	0.52**	0.81**	1													
K_2O	0.87**	0.72**	0.78**	0.68**	0.77**	-0.26	0.83**	0.64**													
P_2O_5	0.2	0.48*	0.04	0.14	0.23	-0.43*	-0.17	0.03	0.26	1											
V	0.79**	0.88**	0.81**	0.89**	0.89**	-0.07	0.79**	0.52**	0.59**	0.31											
Cr	0.74**	0.9**	0.71**	0.80**	0.85**	-0.13	0.72**	0.45*	0.63**	0.54**	0.90**	1									
Ni	0.14	0.03	0.29	0.27	0.18	0.48*	-0.16	-0.02	0.05	-0.31	0.12	-0.07	1								
Cu	0.54**	-0.28	-0.42*	-0.23	-0.34	0.34	0.56**	0.64**	-0.59**	0.19	-0.07	-0.03	-0.1	1							
Zn	0.36*	0.48*	0.5**	0.63**	0.5**	0.52**	-0.39*	-0.14	0.34	0.27	0.62**	0.6**	0.26	0.26	1						
Rb	0.76**	0.612**	0.67**	0.57**	0.66**	-0.15	0.73**	0.48*	0.95**	0.33	0.44*	0.53**	0.12	0.55**	0.37*	1					
Sr	0.69**	-0.41*	0.75**	0.65**	-0.6**	-0.31	0.71**	-0.48*	-0.71**	0.19	-0.35	-0.34	0.37*	0.57**	-0.35	0.73**	1				
Y	0.88**	0.98**	0.83**	0.85**	0.92**	-0.29	0.85**	0.67**	0.70**	0.45*	0.92**	0.9**	0.1	-0.21	0.5**	0.58**	-0.38*	1			
Zr	0.69**	0.94**	0.59**	0.66**	0.78**	-0.41*	0.68**	0.49*	0.55**	0.64**	0.81**	0.87**	-0.13	-0.11	0.43*	0.46*	-0.13	0.91**	1		
Nb	0.9**	.94**	0.9**	0.91**	0.92**	-0.01	0.89**	0.63**	0.74**	0.3	0.88**	0.84**	0.11	-0.31	0.58**	0.62**	0.57**	0.92**	0.82**	1	
Ba	0.9**	0.72**	0.83**	0.70**	0.76**	-0.21	0.86**	0.77**	0.83**	0.11	0.54**	0.53**	0.1	0.67**	0.23	0.76**	0.76**	0.7**	0.51**	0.79**	1

** Correlation is significant at the 0.01 level * Correlation is significant at the 0.05 level

Table 4: Correlation matrix of major and trace element concentrations for the bottom sediments of Al-Mejarma Lagoon. All correlations are significant at the P < 0.01 level (n = 20).

	SiO_2	TiO_2	Al_2O_3	$^tFe_2O_3$	MnO	MgO	CaO	Na_2O	K_2O	P_2O_5	V	Cr	Ni	Cu	Zn	Rb	Sr	Y	Zr	Nb	Ba
SiO_2	1																				
TiO_2	0.98**	1																			
Al_2O_3	0.99**	0.97**	1																		
$^tFe_2O_3$	0.97**	0.96**	0.99**	1																	
MnO	0.99**	0.99**	0.96**	0.97**	1																
MgO	0.7**	0.66**	0.76**	0.80**	0.7**	1															
CaO	-0.99**	-0.9**	0.99**	0.99**	0.98**	0.75**	1														
Na_2O	0.96**	0.93**	0.93**	0.89**	0.93**	0.51*	-0.94**	1													
K_2O	0.97**	0.95**	0.95**	0.93**	0.96**	0.64**	-0.95**	0.89**	1												
P_2O_5	0.88**	0.92**	0.9**	0.91**	0.91**	0.77**	-.9**	0.75**	0.857**	1											
V	0.98**	0.97**	0.99**	0.99**	0.97**	0.75**	-0.98**	0.9**	0.944**	0.89**	1										
Cr	0.95**	0.93**	0.97**	0.97**	0.94**	0.79**	-0.97**	0.87**	0.900**	0.89**	0.96**	1									
Ni	0.93**	0.91**	0.96**	0.98**	0.93**	0.86**	-0.95**	0.81**	0.876**	0.91**	0.96**	0.97**	1								
Cu	-0.053	-0.07	0.016	0.083	-0.045	0.12	0.007	-0.05	-0.198	-0.057	0.06	0.14	0.14	1							
Zn	0.92**	0.9**	0.96**	0.98**	0.93**	0.88**	-0.95**	0.81**	0.87**	0.89**	0.96**	0.96**	0.98**	-0.189	1						
Rb	0.92**	0.9 **	0.92**	0.9**	0.92**	0.68**	-0.91**	0.81**	0.98**	0.84**	0.91**	0.86**	0.86**	-0.237	0.86**	1					
Sr	-0.94**	-0.9**	0.95**	0.95**	0.93**	0.87**	-0.96**	0.83**	-0.91**	.092**	0.93**	0.9**	0.94**	-0.113	0.93**	-0.9**	1				
Y	0.97**	0.98**	0.96**	0.95**	0.97**	0.64**	-0.96**	0.91**	0.95**	0.89**	0.95**	0.91**	0.88**	-0.084	0.88**	0.91**	-0.89**	1			
Zr	0.92**	0.96**	0.9**	0.89**	0.94**	0.55**	-0.91**	0.89**	0.91**	0.82**	0.92**	0.83**	0.82**	-0.145	0.81**	0.86**	-0.83**	0.94**	1		
Nb	0.98**	0.99**	0.98**	0.98**	0.99**	0.72**	-0.98**	0.91**	0.94**	0.93**	0.98**	0.94**	0.94**	-0.028	0.93**	0.91**	-0.93**	0.98**	0.94**	1	
Ba	0.99**	0.97**	0.97**	0.94**	0.98**	0.66**	-0.98**	0.96**	0.97**	0.85**	0.95**	0.92**	0.88**	-0.148	0.88**	0.92**	-0.93**	0.95**	0.92**	0.96**	1

** Correlation is significant at the 0.01 level * Correlation is significant at the 0.05 level

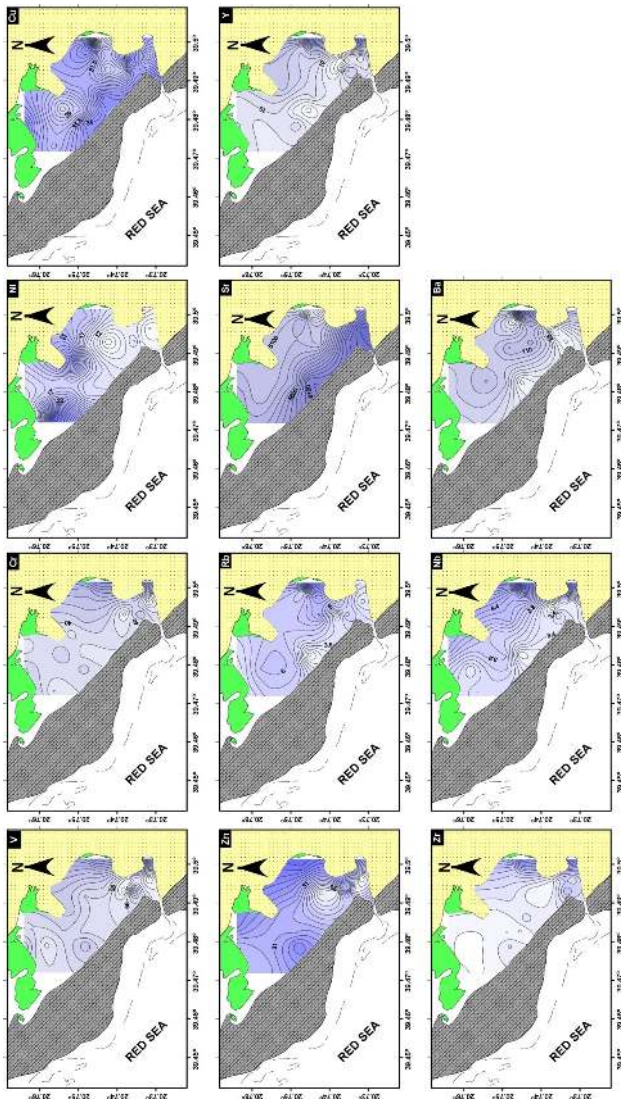

Figure 3: Contour maps showing the spatial distribution of trace elements (µg/g) in the bottom sediments of Al-Shuaiba Lagoon

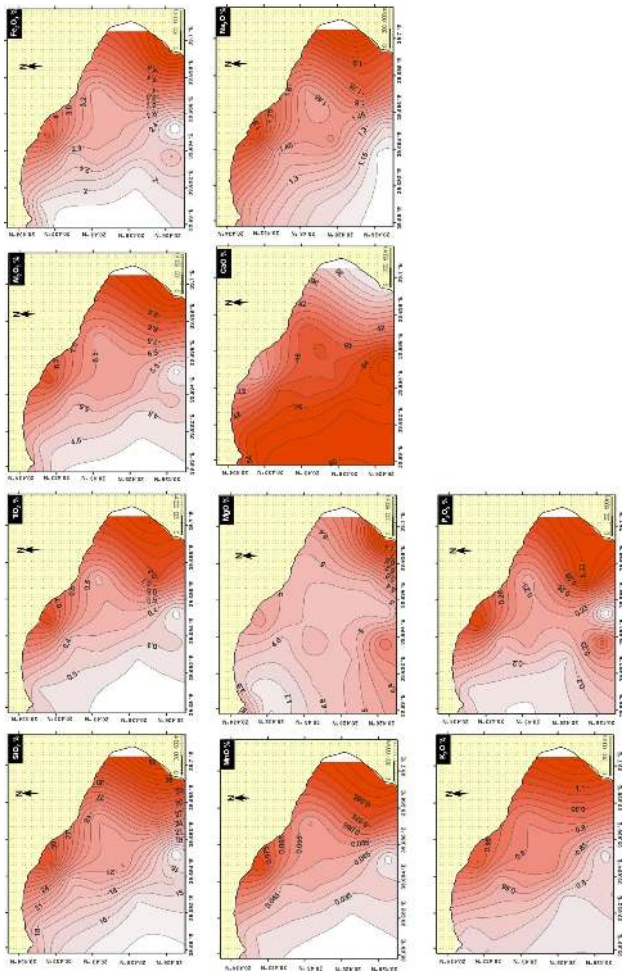

Figure 4: Contour maps showing the spatial distribution of major oxides (%) in the bottom sediments of Al-Mejarma Lagoon

3.2.2 Trace elements

The spatial distribution of trace elements within Al-Shuaiba and Al-Mejarma lagoons displays some similarity with major elements. In the sediments of the SHL, elements such as V, Cr, Rb, Y, Zr, Nb and Ba behave similarly as the continental derived major elements. They show eastward increase in their concentrations (Figs. 3 and 5). The concentration range of these elements are 47-92, 31-65, 1-14, 7-19, 170-498, 3-6 and 62-169 µg/g, respectively (Table1). On the other hand, the concentrations of trace elements except for Sr in the sediments of the SHL increase generally in the shoreward direction (Fig. 3). The concentration of Sr shows a similar behaviour as carbonate related major elements CaO and MgO and its concentration increases in the seaward direction. The concentration of Sr varied in the sediments of Al-Shuaiba from 4114 to 7537 (average; 5581 µg/g) and from 2286 to 6356 (average; 5005 µg/g) in the sediments of Al-Mejarma. The distribution of Ni, Cu and Zn in the sediments of the SHL differs from other investigated trace elements. The concentrations of Ni and Zn display a northward increase, with average concentrations of 15 and 31 µg/g, respectively (Table 1 and Fig. 3). The concentration of Cu increases in the central and NW direction (Fig. 3) varying from 24.08 to 38.22 µg/g with an average of 31.90 µg/g (Table 1).

3.2.3 Geochemical Association

To discriminate different groups of samples having a similar geochemical composition, cluster analysis was employed using the correlation coefficient between all pairs of samples (Fig. 6). The dendrograms show variation in

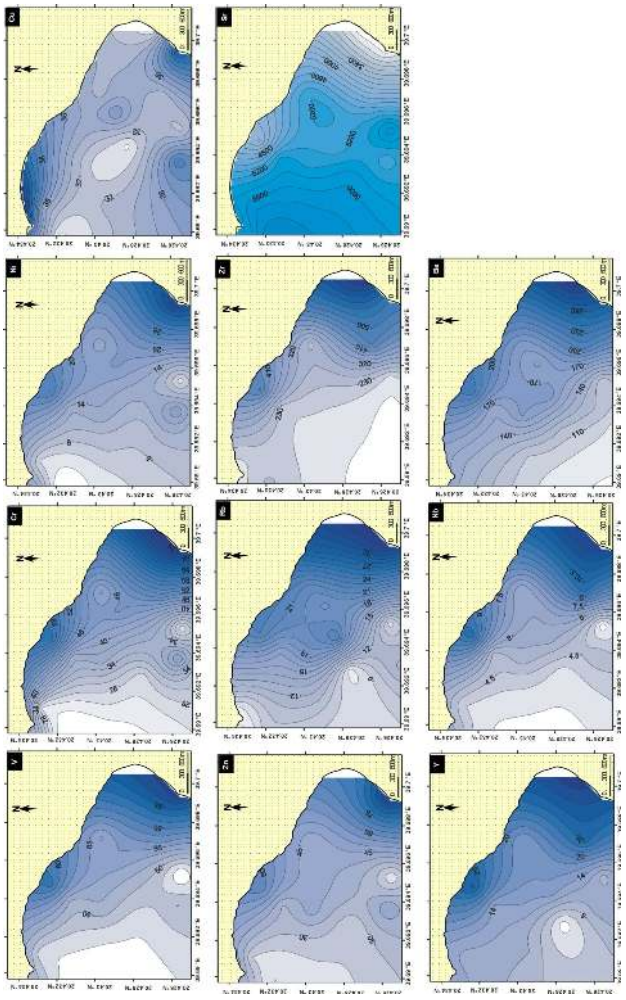

Figure 5: Contour maps showing the spatial distribution of major oxides (%) in the bottom sediments of Al-Mejarma Lagoon

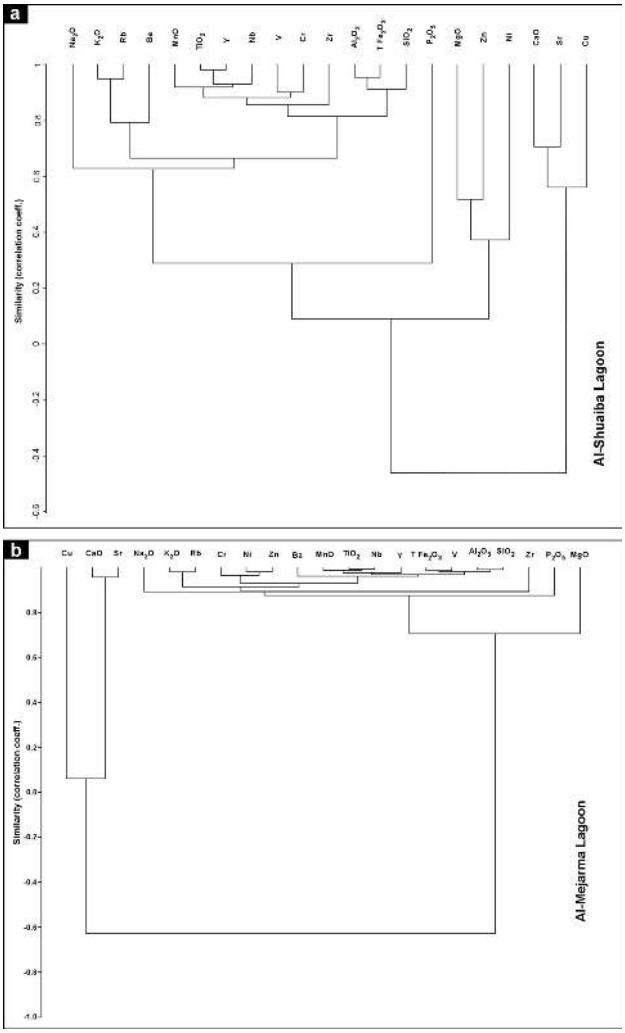

Figure 6: Dendrograms showing the clustering of elements in the Al-Shuaiba (a) and Al-Mejarma (b) lagoons

the degree of similarity and difference among trace and major elements in the two lagoons. In the sediments of the SHL, the dendrogram shows some geochemical associations; carbonate related elements (CaO-Sr), silicates (Al_2O_3-Fe_2O_3-SiO_2), Feldspars (K_2O-Rb-Ba) and heavy minerals (V-Cr-Zr, TiO_2-Y-Nb). For the MJL sediments, the dendrogram shows some similarities and variations with that of SHL. The geochemical associations in the sediments of MJL include carbonate related elements (CaO-Sr), silicates (Al_2O_3- SiO_2), feldspars (K_2O-Rb) and heavy minerals (TiO_2-Nb-Y). The dendrogram obtained for Al-Mejarma shows differences on geochemical behaviour for some elements; CaO is less related to MgO, and Cr and Na are not clearly associated to any geochemical group.

3.2.4 Elemental Interrelationships

Elemental interrelationships (Tables 3 and 4 and Figure 7) in the sediments of Al-Shuaiba show significant positive correlation (r > 0.8) between SiO_2 and TiO_2, Al_2O_3, Fe_2O_3, MnO, Na_2O and K_2O. SiO_2 displays a significant positive correlation (Table, Figure) with V (r = 0.79), Cr (r = 0.74), Rb (r = 0.76), Y (r = 0.88), Nb and Ba (r = 0.9) in the sediments of Al-Shuaiba. In the sediments of Al-Mejarma, SiO_2 displays a significant positive correlation (r > 0.85) with major elements except CaO and MgO. Similarly, it shows significant positive correlation (r > 0.9) with most trace elements except Cu and Sr. CaO displays significant positive correlation with Sr in the sediments of Al-Shuaiba (r =0.71) and Al-Mejarma (r = 0.9) lagoons. Barium (Ba) correlates positively with K_2O and Rb in the sediments of Al-Shuaiba (r = 0.83 and 0.76, respectively) and in Al-Mejarma (r = 0.

0.97 and 0.92, respectively) suggests that Ba is mainly derived from a terrestrial source, possibly K-feldspar. SiO_2 behave as Al_2O_3 suggesting that most of SiO_2 are of terrigenous origin. Al displays strong positive correlation with Ti suggesting that most Ti is associated with clay minerals. Fe_2O_3-V may indicate the accumulation of V in Fe-minerals by adsorption. The strong positive correlation of Fe_2O_3 with Na_2O, MnO, V, Cr, Ni and Zn suggests that these metals are closely associated with Fe oxyhydroxides and Fe-rich minerals such as hornblende [33, 34].

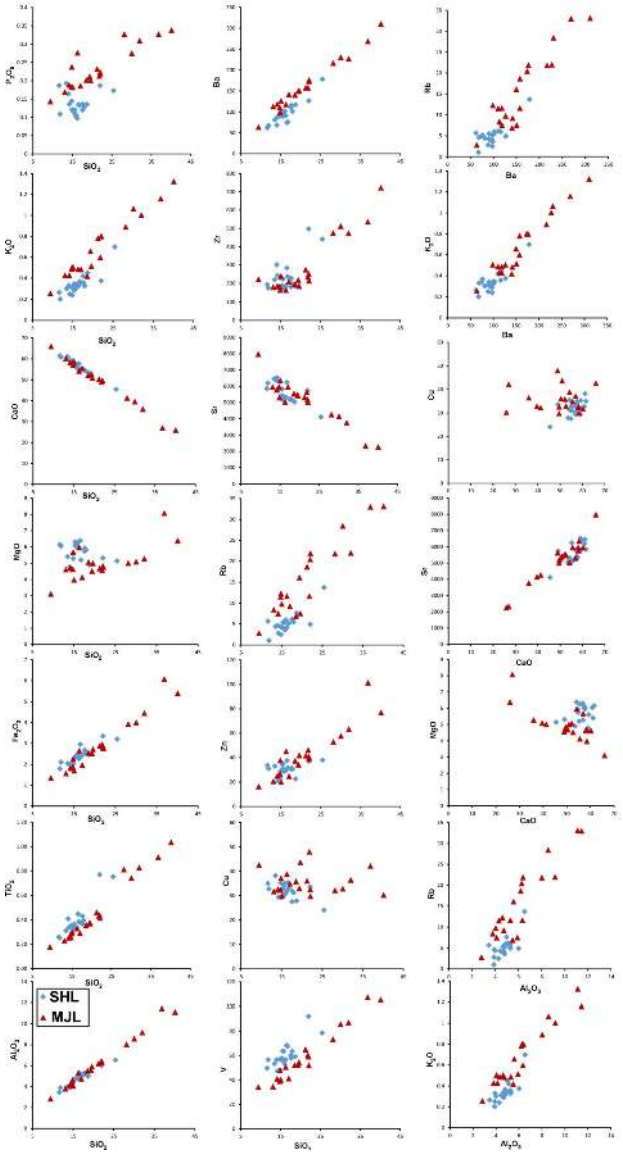

Figure 7: Relationship of SiO_2, Al_2O_3, CaO and Ba with the major and trace elements in the sediments of Al-Shuaiba and Al-Mejarma lagoons

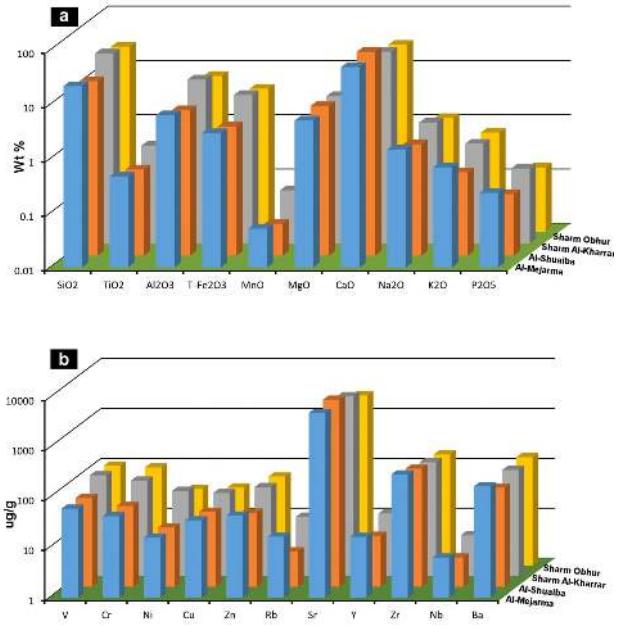

Figure 8: Histogram showing the average concentrations of major (a) and trace (b) elements on the sediments of Al-Shuaiba and Al-Mejarma lagoons relative to the Sharm Al-Kharrar (Rabigh area; Basaham et al. [11]) and Sharm Obhur (Jeddah City; Ghandour et al. [9]).

The average concentrations of the major and trace elements in the sediments of Al-Shuaiba and Al-Mejarma lagoons were correlated with the average chemical composition of the bottom sediments of two Red Sea coastal lagoons; Sharm Obhur, Jeddah [9] and Sharm Al-Kharrar, Rabigh area. The correlation shows that the land derived major and trace elements are more abundant in the bottom sediments of Sharm Al-Kharrar followed by Sharm Obhur than in Al-Shuaiba and Al-Mejarma lagoonal sediments (Figure 8). On the other hands, the carbonate related elements (CaO, MgO and Sr) are more abundant in the sediments of Al-Shuaiba followed by Al-Mejarma (Figure 8).

4 Discussion

The carbonate-dominated SHL and MJL bottom sediments are consistent with the extremely hot and arid climatic conditions prevail in the area. The distribution and concentrations of the major oxides and trace elements in the sediments of the two lagoons display somewhat remarkable variations reflecting the spatial variations in the composition and grain size of the calcareous skeletal remains,

lagoonal bottom conditions and organic matter content. These variations may be attributed to the variations in the lagoonal morphology and the connection with the Red Sea.

The composition of skeletal remains and the lagoonal hydrodynamics with the relevant grain size play a significant role in the spatial distribution of the carbonate related elements (CaO, MgO and Sr). CaO and Sr are closely related and display similar distribution pattern. They have strong negative correlations with the land-derived elements suggesting that the two elements were derived from a similar source that is independent of alumino-silicate and other land-derived minerals and related to the biogenic origin [35].

The concentrations of CaO, MgO and Sr in the sediments of SHL are closely related to the mineralogical composition which in turn is correlated with the hydrodynamically controlled grain size and the dominant skeletal remains. Corals and molluska of dominantly aragonitic composition dominate the coarse-grained inlet channel sediments. These sediments are highly enriched in CaO and Sr. On the other hands, MgO shows high concentrations in the fine-grained sediments near the northern and western shorelines. These sediments contain abundant red algae and benthic foraminiferal remains, which is consistent with the dominance of high-magnesium calcite. The concentration of $MgCO_3$ in the skeletal remains of corals and molluska ranges between 0.1 and 0.2 % [36], whereas it ranges in calcareous algae between 8.3 to 35 % [37].

Similarly, the concentrations of CaO and Sr in the sediments of the MJL decrease in a landward direction, whereas the MgO concentration increases towards the fine grain dominated southern and southeastern nearshore area. The higher concentrations of MgO towards the southern shoreline is consistent with the high content of high-magnesium calcite over aragonite. MgO is favoured over Sr in the calcite lattice and Sr is favoured over MgO in aragonite lattice. The regression for Sr-CaO and MgO-CaO show strong positive correlation for the former and poor to negative correlation for the second indicating that calcite was the main carbonate minerals in the SHL and MJL bottom sediments.

The land-derived major oxides (SiO_2, TiO_2, Al_2O_3, Fe_2O_3 and MnO) and trace elements (V, Cr, Zr, Rb, Y and Nb) display a generally similar distribution pattern. Their concentrations in contrast to the carbonate related elements increase generally in the sheltered and low energy nearshore areas. They are mostly concentrated in fine-grained sediments that is consistent with aeolian transportation. In the sediments of the SHL, higher concentrations of the land-derived elements were recorded near the eastern shoreline than the western shoreline. This is attributed to the limited dilution by autochthonous biogenous and hydrogenous calcareous sediments and the allochthonous carbonate sediments derived from the nearby fossil barrier reef bordering the lagoon from the west. In the MJL, the concentrations of the land-derived elements show regular landward increase because the biogenic calcareous sediments are common in the relatively deeper seaward parts.

4.1 Lagoonal Bottom Conditions

Earlier studies [6, 16] suggested that the bottom of the SHL experiences stagnation and anoxic conditions particularly in areas that are enriched in organic matter. They attributed the stagnant conditions to the limited water exchange with the Red Sea and the hypersalinity because of arid climate. They further linked this stagnant condition with the formation of pyrite. Geochemical data presented here does not support variation in the bottom redox conditions. The concentrations of the Al-normalized redox-sensitive trace elements (V and Cr) show no obvious enrichment within the lagoon. The V/Cr ratio has been employed to define the oxic-suboxic conditions; oxic-dysoxic and dysoxic-anoxic boundaries correspond respectively to V/Cr ratios of 2 and 4.25, respectively [38, 39]. The V and Cr tend to be more soluble under oxidizing conditions and less soluble and enriched under reducing conditions [40, 41]. In the present study, the V/Cr values are generally less than 2 all over the lagoon suggesting that the bottom conditions of the two lagoons are well oxygenated. In addition, oxic conditions are normally developed in the well-circulated shallow water environment due to frequent exchange with the overlying oxic atmosphere. Generally, the shallow depths of the two lagoons along with the active wind and tidal stirring allow well mixing of waters of relatively high salinity and temperature and prevent the development of stratification.

Pyrite if present in the bottom sediments of Al-Shuaiba Lagoon has been attributed to the presence of dysoxic to anoxic bottom conditions [16]. However, pyrite can be formed under both anoxic and oxic conditions. Under anoxic condition, the formation of pyrite is enhanced by organic content and bacterial sulfate reduction [35]. Pyrite on the other hand, can be formed but with low rate under oxic condition below the sediment-water interface. Oxidation of organic matter inhibits bacterial sulfate reduction and thus the formation of H_2S which prevents the formation of pyrite. Under oxic conditions, reworking by bioturbation lead to oxidation of pyrite to Fe oxides [42].

5 Conclusions

The geochemical and mineralogical composition of bottom sediments of two Red Sea carbonate-dominated coastal lagoons; Al-Shuaiba and Al-Mejarma are determined. The sediments of the two lagoons show slight variations in their chemical and mineralogical composition reflecting the influence of the lagoonal hydrodynamic energy and its control on sediment grain size and the limited exchange with seawater.

1. The bottom sediments consist mainly of carbonate minerals aragonite and high and low-Mg calcite and the non-carbonate minerals are dominated by quartz along with rare feldspars, clay minerals, mica and amphiboles. The chemical composition of the bottom sediments of the two lagoons is slightly different, with the sediments of Al-Shuaiba yielded higher average concentrations of carbonate related elements (CaO, MgO and Sr).
2. The spatial distribution of CaO, MgO and Sr is controlled mainly by hydrodynamic energy the relevant grain size. In areas of high energy such as inlet channels, skeletal remains of corals and molluska of dominantly aragonitic composition dominate the sediments with high content of CaO and Sr. On the other hands, the areas of low hydrodynamic energy, the fine grained sediments contain abundant calcareous algae and foraminifera with high Mg calcite and consequently relatively high MgO concentrations.
3. Trace elements are abundant in areas having high mud and organic carbon content suggesting that trace elements are adsorbed to, or complexes with organic debris and/or clay minerals.
4. Based on elemental correlations, cluster analysis differentiates 4 geochemical groups: carbonate related elements (CaO-Sr), silicates (Al_2O_3-Fe_2O_3-SiO_2), Feldspars (K_2O-Rb-Ba) and heavy minerals (V-Cr-Zr, TiO_2-Y-Nb) for the sediments of Al-Shuaiba Lagoon, and for the Al-Mejarma Lagoon are carbonate related elements (CaO-Sr), silicates (Al_2O_3- SiO_2), feldspars (K_2O-Rb) and heavy minerals (TiO_2-Nb-Y).
5. The geochemical data indicate that the bottom of the lagoon was fully oxygenated regardless the high organic matter content. The depletion of redox sensitive trace elements (V and Cr) and the low values of V/Cr ratio suggest that bottom waters were oxic.Shallow water depths of the two lagoons and the continuous water stirring by the action of wind and tide prevent water stratification and allow mixing of surface and bottom waters.

Acknowledgements This project was funded by the Deanship of Scientific Research (DSR) at King Abdulaziz University, Jeddah, under grant no. G-76-150-1438. The authors, therefore, acknowledge with thanks DSR for technical and financial support. The authors would like to thank the reviewers and the editor for the constructive comments and for editorial improvement of the manuscript. Thanks extend to Prof. Athar A. Khan (KAU) for language editing.

References

[1] Migani F., Borghesi F., Dinelli E.,. Geochemical characterization of surface sediments from the northern Adriatic wetlands around the Po river delta. Part I: Bulk composition and relation to local background. J. Geochem. Explor., 2015, 156,72-88 http://dx.doi.org/10.1016/j.gexplo.2015.05.003

[2] Capolupo M., Franzellitti S., Kiwan A., Valbonesi P., Dinelli E., Pignotti E., Birke M., Fabbri E., A comprehensive evaluation of the environmental quality of a coastal lagoon (Ravenna, Italy): Integrating chemical and physiological analyses in mussels as a biomonitoring strategy. Science of the Total Environment, 2017 598, 146-159

[3] Chandra A.S., Rath P., Chandra P.U., Kumar P.P., Bramha S., Application of sequential leaching, risk indices and multivariate statistics to evaluate heavy metal contamination of estuarine sediments: Dhamara Estuary, East Coast of India. Environ. Monit. Assess., 2013, 185, 6719-6737

[4] Borghesi F., Migani F., Dinelli E., Geochemical characterization of surface sediments from the northern Adriatic wetlands around the Po River delta. Part II: aqua regia results. J. Geochem. Explor., 2016, 169, 13-29

[5] Petti M., Bosa S., Pascolo S., Lagoon Sediment Dynamics: A Coupled Model to Study a Medium-Term Silting of Tidal Channels. Water, 2018, 10 (569), 1-19

[6] Rasul N.M.A.,. Lagoon sediments of the Eastern Red Sea: distribution processes, pathways and patterns. In: Rasul N.M.A., Stewart I.C.F. (eds) The Formation, Morphology, Oceanography and Environment of a Young Ocean Basin, 2015, 281–316. Springer, Heidelberg

[7] Durgaprasada Rao N.V.N., Al-Imam O.A.O., Behairy A.K.A., Early mixed-water dolomitization in the Pleistocene reef limestones, west coast of Saudi Arabia. Sed Geol., 1987, 53, 231–245

[8] Rabaa S.M.A., Geomorphological characteristics of the Red Sea coast with special emphasis on the formation of Marsas in the Sudan. In: Proceedings of a Symposium on Coastal and Marine Environments of the Red Sea, Gulf of Aden and Tropical Western Indian Ocean. 1980, 53–72. University of Khartoum, Khartoum, Sudan

[9] Ghandour I.M., Basaham S., Al-Washmi A., Masuda H., Natural and anthropogenic controls on sediment composition of an arid coastal environment: Sharm Obhur, Red Sea, Saudi Arabia. Environ Monit Asses., 2014, 186, 1465–1484

[10] Basaham A.S., Mineralogical and chemical composition of the mud fraction from the surface sediments of Al-Kharrar, a Red Sea coastal lagoon. Oceanologia, 2008, 50, 557–575

[11] Basaham A.S., El Sayed M.A., Ghandour I.M., Masuda H., Geochemical background for the Saudi Red Sea coastal systems

and its implication for future environmental monitoring and assessment. Environ Earth Sci., 2015, 74, 4561–4570

[12] Youssef M. , El-Sorogy A., Environmental assessment of heavy metal contamination in bottom sediments of Al-Kharrar lagoon, Rabigh, Red Sea, Saudi Arabia. Arabian Journal of Geosciences, 2016, DOI 10.1007/s12517-016-2498-3

[13] Hariri M.S.B., Abu-Zeid R.H., Factors influencing heavy metal concentrations in the bottom sediments of the Al-Kharrar Lagoon and Salman Bay, eastern Red Sea coast, Saudi Arabia. Arab. J. Geosci., 2018, https://doi.org/10.1007/s12517-018-3838-2

[14] Badr N.B.E., El-Fiky A.A., Mostafa A.R., Al-Mur B.A., Metal pollution records in core sediments of some Red Sea coastal areas, Kingdom of Saudi Arabia. Environ Monit Assess. 2009, 155, 509–526

[15] Al-Washmi H.A., Sedimentological aspects and environmental conditions recognized from the bottom sediments of Al-Kharrar Lagoon, Eastern Red Sea coastal plain, Saudi Arabia. J King Abdulaziz Univ Mar. Sci., 1999, 10, 71-87.

[16] Al-Washmi H.A. Gheith A.M., Recognition of Diagenetic Dolomite and Chemical Surface Features of the Quartz Grains in Coastal Sabkha Sediments of the Hypersaline Shuaiba Lagoon, Eastern Red Sea Coast, Saudi Arabia. J King Abdulaziz Univ Mar. Sci., 2003, 14, 101-112

[17] Abu-Zied R.H., Bantan R.A., El Mamoney M.H., Present environmental status of the Shuaiba Lagoon, Red Sea Coast, Saudi Arabia. J King Abdulaziz Univ. Mar. Sci., 2011, 22(2), 159–179

[18] Ghandour I.M., Al-Washmi, H., Textural and mineralogical heterogeneities in coastal lagoon sediments: Al-Mejarma Lagoon, Red Sea, Saudi Arabia. Journal of King Abdulaziz University, Marine Sciences 2012, 23 (1), 109–125

[19] Abu-Zied R.H., Bantan R.A., Hypersaline benthic foraminifera from the Shuaiba Lagoon, eastern Red Sea, Saudi Arabia: Their environmental controls and usefulness in sea-level reconstruction. Mar Micropaleont., 2013, 103, 51–67. doi:10.1016/j.marmicro. 2013.07.005

[20] Kjerfve B., Coastal Lagoons. In: Kjerfve B., (ed) Coastal Lagoon Processes. Elsevier Oceanography Series, 1994, 1-8

[21] Skipwith P., The Red Sea and coastal plain of the Kingdom of Saudi Arabia. Tech. Report TR-1073-I, Diect. Gen Miner. Res, Saudi Arabia, 1973, 149 pages

[22] Al-Sayari S.S., Zötl J.G., Quaternary period in Saudi Arabia. Springer-Verlag, Wein, New York, 1978, 335 pages

[23] Sofianos S. S., Johns W.E., Murray S.P., Heat and freshwater budgets in the Red Sea from direct observations at Bab el Mandeb. Deep Sea Res. II, 2002, 49, 1323-340

[24] Lisitzin, E., Sea-Level Changes. Elsevier Oceanogr. Ser.8. Elsevier Sci, Publ. Co., Amsterdam, Oxford, New York, 1974, 286 pages

[25] Ahmed F.C., Khomayis H.S., Turki A.J., Rasul N.M., A multidisciplinary oceanographic study of three environmentally sensitive sites along the Saudi Arabian coast of the Red Sea. Res Council, King Abdulaziz Univ, Final Report, Sci., 2002, 82 pages

[26] Ahmed F.C., Sultan S.A.R., The effect of meteorological forcing on the flushing of Shuaiba Lagoon on the eastern coast of the Red Sea. J King Abdulaziz Univ Mar. Sci., 1992, 3,3–9

[27] Al-Barakati A.M.A., Application of 2-D tidal model, Shuaiba Lagoon, eastern Red Sea coast. Can J Comput Math Nat Sci Med 2010, 1, 9–20

[28] Hardy R., Tucker M., X-ray powder diffraction of sediments. In: Tucker M., (ed) Techniques in Sedimentology. Blackwell Science, Cambridge, 1988, 191–228,

[29] Moore D.M., Reynolds, R.C., X-ray Diffraction and the Identification and Analysis of Clay Minerals. Oxford Univ. Press, 1989, 332 pages

[30] Tawfik H.A., Ghandour I.M., Maejima W., Armstrong-Altrin, J.S., Abdel-Hameed A.T.,. Petrography and geochemistry of the siliciclastic Araba Formation (Cambrian), east Sinai, Egypt: implications for provenance, tectonic setting and source weathering. Geological Magazine, 2017, 154 (1), 1-23. DOI: https://doi.org/10.1017/S0016756815000771

[31] Vitturi L.M., Mounarou, E., Pistolato M., Rampazzo G., Geochemistry of recent sediments in the Lagoon of Venice. Rendiconti Della Societa Italiana Di Mineralogia E Petrologica, 1987, 42, 59-72

[32] Hammer O., Harper D.A.T., Ryan P.D., PAST: Palaeontological statistics software package for education and data analysis. Palaeontologia Electronica, 2001, 4(1), 9pp

[33] Taylor G., Eggleton R.A., Regolith Geology and Geomorphology. John Wiley & Sons Ltd, Chichester. 2001, 375 pages

[34] Daesslé L.W., Rendón-Márquez G., Camacho-Ibar V.F., Gutiérrez-Galindo E.A., Shumilin E., Ortiz-Campos E., Geochemistry of modern sediments from San Quintín coastal lagoon, Baja California: Implication for provenance. Revista Mexicana de Ciencias Geológicas, 2009, 26 (1), 117-132

[35] Rubio B., Nombela M.A. Vilas F., Geochemistry of major and trace elements in sediments of the Ría de Vigo (NW Spain): an assessment of metal pollution. Marine Pollution Bulletin, 2000, 40, 968–980

[36] Speer J.A., Crystal chemistry and phase relations of orthorhombic carbonates. In: Reeder R.J. (ed) Carbonates: Mineralogy and Chemistry. Rev. Mineral. Mineral. Soc. Am., Washington, DC, 1983, 11, 145–190

[37] Mackenzie F.T., Bischoff W.B., Bishop F.C., Loijens M., Schoonmaker J., Wollast R., Magnesian calcites: Low-temperature occurrence, solubility and solid-solution behavior, In: Reeder R.J. (ed), Carbonates Mineralogy and Chemistry. 1983, 97-144

[38] Jones B., Manning D. A. C., Comparison of geochemical indices used for the interpretation of palaeoredox conditions in ancient mudstones: Chemical Geology, 1994, 111 (1-4), 111-129

[39] McManus J., Berelson W.M., Severmann S., Poulson R.L., Hammond D.E., Klinkhammer G.P., Holm C., Molybdenum and uranium geochemistry in continental margin sediments: Paleoproxy potential. Geochimica Et Cosmochimica Acta, 2006, 70 (18), 4643-4662

[40] Algeo T.J., Maynard J.B., Trace element behavior and redox facies in core shales of Upper Pennsylvanian Kansas-type cyclothems: Chemical Geology, 2004, 206, 289–318. doi: 10.1016/j.chemgeo.2003.12.009

[41] Hetzel A., März C., Vogt C., Brumsack H.J., Geochemical environment of Cenomanian - Turonian black shale deposition at Wunstorf (northern Germany): Cretaceous Research, 2011, 32 (4), 480–494. doi: 10.1016/j.cretres.2011.03.004

[42] Raiswell R., Buckley F., Berner R.A., Anderson T.F., Degree of pyritization of iron as a paleoenvironmental indicator of bottom-water oxygenation. Journal of Sedimentary Petrology, 1988, 58(5), 812–819